

## P5.3 VALIDATION OF SATELLITE-DERIVED LIQUID WATER PATHS WITH GROUND-BASED MICROWAVE RADIOMETERS FOR VARIOUS CLOUD REGIMES

Mandana M. Khaiyer\*, Rabindra Palikonda, Michele L. Nordeen, J. Kirk Ayers  
Analytical Services & Materials Inc., Hampton, VA

Patrick Minnis  
Atmospheric Sciences, NASA-Langley Research Center, Hampton, VA

R.F. Arduini  
Science Applications International Corporation, Hampton, VA

### 1. INTRODUCTION

Cloud liquid water path (LWP) is an important climatic variable, especially for validating climate models and possibly numerical weather model forecasts. Satellites provide the advantage of widespread coverage of this and other cloud characteristics, while ground-based microwave radiometers (MWR) can only provide point measurements. To provide high temporal resolution coverage of large areas, the VISST (Visible Infrared Solar Split-Window Technique) is utilized to derive LWP from the suite of Geostationary Operational Satellites (GOES), providing coverage over the Pacific and Atlantic Oceans, and the continents of North America and Australia. These extensive areas are covered by clouds from different continental and marine regimes, and confidently using one specific satellite retrieval technique to derive all of them requires validation in those regimes.

Comparisons of VISST-retrieved LWP are made to MWR retrievals from various sites. Three are Atmospheric Radiation Measurement (ARM) sites, covering both the tropics and the mid-latitudes. The former category is represented by the Tropical Western Pacific (TWP) site located at Manus (2.058°S, 147.425°E). The latter includes the Southern Great Plains (SGP) site in Oklahoma (36.61°N, 97.49°W), and the ARM Mobile Facility (AMF) at Pt. Reyes, California (38.03°N, 122.98°W). Since these sites provide only a sampling of information over their respective regions, satellite-derived cloud retrievals can provide cloud property information over the widespread areas where ground-based data is unavailable.

### 2. METHODOLOGY

During daytime, the data are analyzed with the VISST, which is an updated version of the methodology described by Minnis et al. (1995b). The cloud mask algorithm of Trepte et al. (1999) classifies each pixel as

clear or cloudy, employing data from the 0.65, 3.9, 10.8, and 12.0  $\mu\text{m}$  channels. For each cloudy pixel, the VISST uses those same radiances to estimate cloud phase, effective temperature, effective height, optical depth  $\tau$ , effective particle size  $r_e$ , and liquid or ice water path. VISST-determined LWP is from retrievals of cloud optical depth and droplet effective radius, based on matching visible reflectance and infrared radiance observations with theoretical model estimates of the same variables. This procedure uses an assumed droplet size distribution over a range of effective radii. Cloud-top height and thickness are also derived using empirical methods. At night and near the terminator, the visible channel is unusable, so the cloud height and temperature and a crude estimate of optical depth are estimated using the solar-infrared infrared split-window technique (SIST; Minnis et al. 1995b).

VISST retrievals were performed on GOES data for 1-degree boxes surrounding the 5 sites. Cloud properties were retrieved from GOES-9 data over Manus covering the period May – December 2003. The European Center for Medium Range Forecasting (ECMWF) product was used for temperature and humidity profiles. The mid-latitude sites used Rapid Update Cycle (RUC) hourly model analyses. GOES-8 data taken during 2002 were used over the SGP central facility (SCF), and GOES-10 data were analyzed over Pt. Reyes were completed for the period when the AMF was located there: mid-February through mid-September 2005.

To determine the influence of droplet size distribution width on the retrievals, the data were analyzed using eight separate reflectance models employing different droplet size distribution variances ( $V_{\text{eff}} = 0.01, 0.02, 0.05, 0.10, 0.15, 0.20, 0.25$  and  $0.30$ ). The “control” effective variance used in this study is 0.10, but varying this parameter may allow for more accurate LWP retrievals for differing cloud regimes. Preliminary studies indicate that some of the bias in VISST-derived LWP is due to scattering angle dependencies and possibly 3-D effects of clouds (Ayers et al., 2005), while some of the bias can be accounted for by variations in  $V_{\text{eff}}$  (Arduini et al, 2005).

---

\* *Corresponding Author Address:* Mandana M. Khaiyer, AS&M, Inc., 1 Enterprise Parkway Hampton, VA 23666; E-mail: [m.m.khaiyer@larc.nasa.gov](mailto:m.m.khaiyer@larc.nasa.gov)

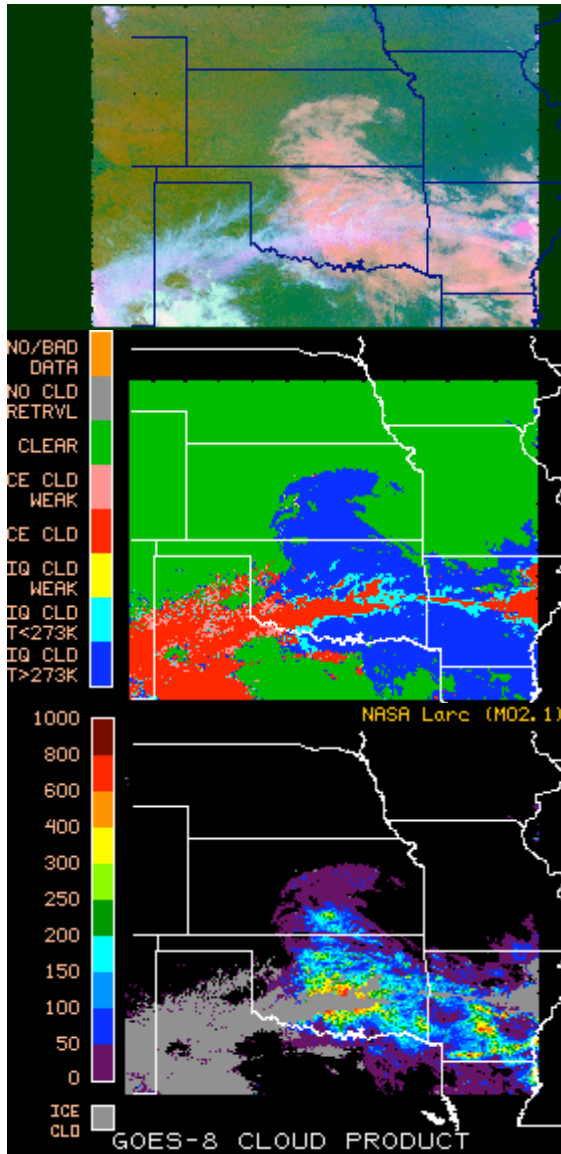


**Figure 1.** GOES-8 imagery and VISST retrievals from 1715 UTC 23 April 2002: a) RGB composite where Red= visible ( $0.65 \mu\text{m}$ ), Green = brightness temperature difference of  $3.9$  and  $11 \mu\text{m}$ , and Blue= $11 \mu\text{m}$  temperature; and VISST-derived b) cloud phase, c) LWP retrievals.

The validation datasets include ground-based MWR retrievals from available ARM instruments at Manus, the SGP, and Pt Reyes. Daytime VISST cloud properties, including amounts, cloud temperatures, and LWP, were averaged over all pixels within a 10- and 20-km radius of the site and are compared with 30-min averages of MWR LWP centered on the GOES retrieval times. MWR LWP averages were used if there were at least 85 quality-checked observations within the time window, including absence of a wet window, no value of liquid  $< -40 \text{ g/m}^2$  and sky infrared temperature  $> 100 \text{ K}$  (if available). MWR LWP averages were not used if standard deviations were  $> 600 \text{ g/m}^2$ .

### 3. RESULTS

Figure 1 shows a) the GOES-8 RGB composite (created from visible and infrared imagery) with the corresponding b) cloud phase and c) LWP retrievals from VISST at 1715 UTC April 23, 2002. This day was characterized by persistent stratus. The cloud features include a stratus deck in the vicinity of the SCF, and some overlying high ice cloud south of the site. The magnitude of LWP for the stratus deck covers a wide range; the central regions of the deck are characterized by a LWP of  $50\text{-}200 \text{ g/m}^2$ .

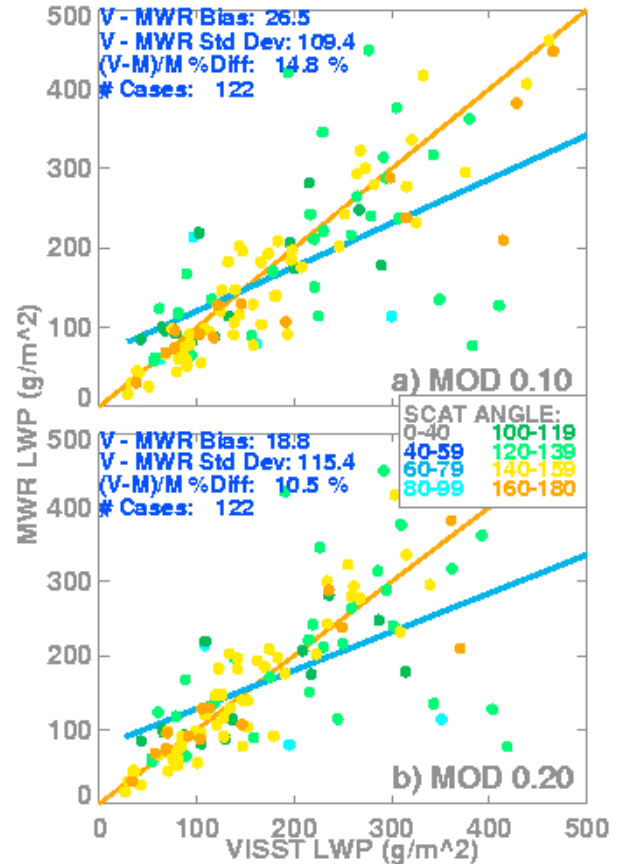


**Figure 2.** Scatterplot of SGP VISST-derived vs ARM MWR-derived LWP for a)  $V_{\text{eff}} = 0.10$ , and b)  $V_{\text{eff}} = 0.20$ . One-to-one line is tan, and line fit is turquoise. Scattering angles are color-coded according to the legend.

While the general cloud pattern is adequately captured in the VISST retrievals, evaluation of the robustness of these results requires validation with ground-based MWR LWP values. The VISST- and ARM MWR-derived LWP at the SCF are compared in Fig. 2 using data for 122 100% warm cloud cases taken at solar zenith angles (SZA)  $< 80^\circ$ . The control case (Fig. 2a) with  $V_{\text{eff}} = 0.10$  yields a bias of  $26.5 \text{ g/m}^2$ , a standard deviation ( $\sigma$ ) of  $109.4 \text{ g/m}^2$ , and a % difference (%D) of 14.8%. The minimum bias is found for the  $V_{\text{eff}} = 0.20$  case (Fig. 2b), where the value decreased to  $18.8 \text{ g/m}^2$  (10.5% difference). However,  $\sigma$  increased to

115.4  $\text{gm}^{-2}$  in this instance. The bias was also low, at 19.5  $\text{gm}^{-2}$  (10.9% difference), for the  $V_{\text{eff}} = 0.01$  case (not pictured), and  $\sigma$  also decreased to 103.7  $\text{gm}^{-2}$ . The largest errors occur at the smallest observed scattering angles.

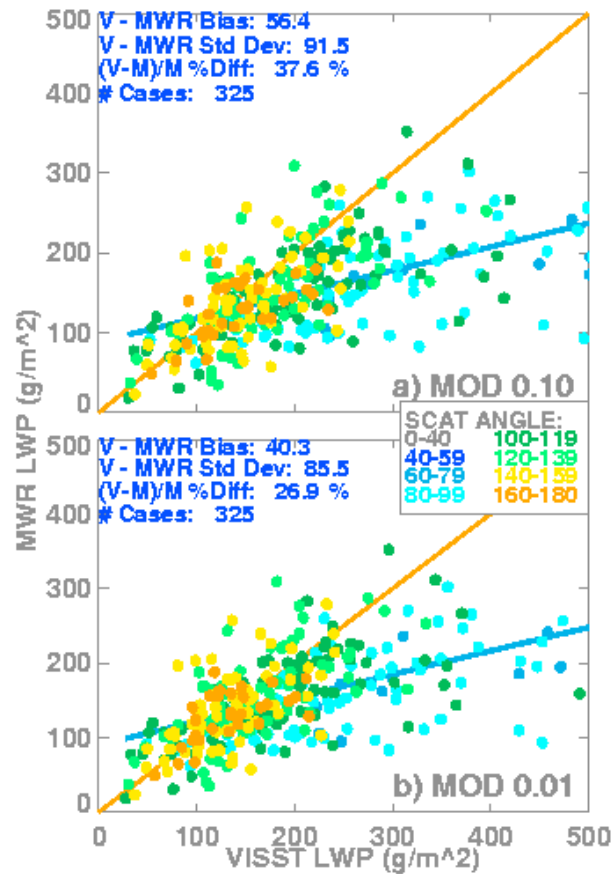


**Figure 3.** As in Fig. 2, but for Pt. Reyes.

Figure 3 shows a scatterplot of the ARM MWR LWP compared to the VISST-derived LWP for 325 data pairs over the Pt. Reyes deployment site, from 100% warm cloud cases having  $\text{SZA} < 80^\circ$ , for the  $V_{\text{eff}} = 0.10$  “control” case (Fig. 3a) and the  $V_{\text{eff}} = 0.01$  case (Fig. 3b). The bias and standard deviation of the differences are smaller for the narrower size distribution; for  $V_{\text{eff}} = 0.01$ , the bias is 40.3  $\text{gm}^{-2}$ ,  $\sigma = 85.5 \text{ gm}^{-2}$ , and %D = 26.9%. For the corresponding  $V_{\text{eff}} = 0.10$  the bias is 56.4  $\text{gm}^{-2}$ ,  $\sigma = 91.5 \text{ gm}^{-2}$ , and %D = 37.6%. All retrievals using  $V_{\text{eff}} < 0.10$  have smaller biases/standard deviations when compared to the control case, whereas those greater than 0.10 have larger differences. The LWP at scattering angles from  $60^\circ$ - $79^\circ$  appear to show the greatest improvement in the Pt. Reyes cases.

The tropics yield a different result as shown in the Manus comparison in Fig. 4, for 17 cases. In this instance, 80% warm cloud was allowed for the comparison as broken cumulus are more common than

stratus for this site. The control case of  $V_{\text{eff}} = 0.10$  (Fig. 4a) yielded a bias of  $-9.8 \text{ gm}^{-2}$  (-12.2% difference), and  $\sigma 49.3 \text{ gm}^{-2}$ . The standard deviations were small in all cases, but these numbers were smallest for the  $V_{\text{eff}} = 0.25$  case (Fig. 4b), where

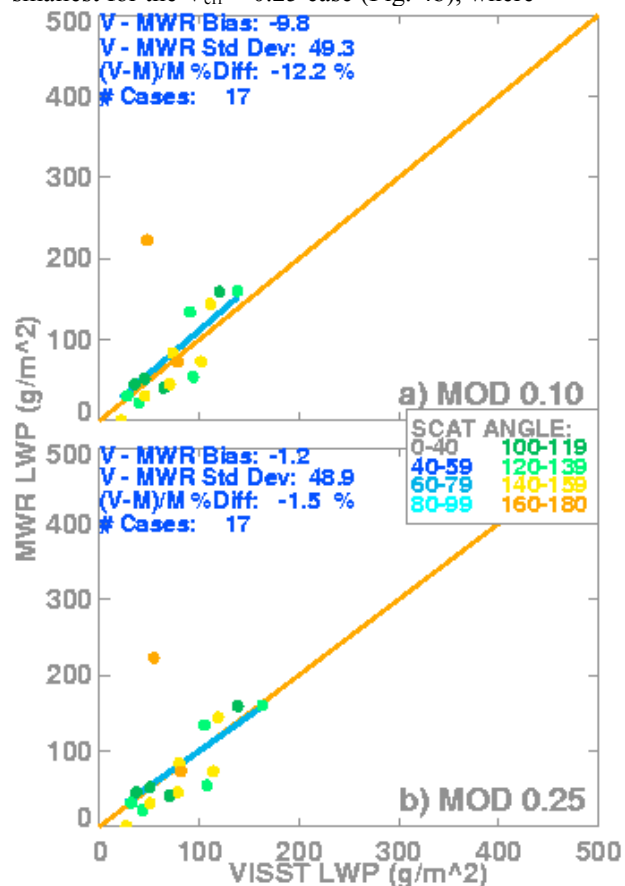


**Figure 4.** As in Fig. 2, but for Manus.

the bias is  $-1.2$  (%D =  $-1.5\%$ ) and  $\sigma$  is 48.9  $\text{gm}^{-2}$ . Over Manus, there are too few points for making any definitive conclusions, although the preliminary results are encouraging.

#### 4. DISCUSSION

The results in Figs. 2 and 3 indicate that the VISST-derived LWP values are close to their ARM-retrieved counterparts at the SGP and Pt. Reyes sites, except at certain scattering angles. Because the scattering angle depends on the time of day for geostationary satellite observations, the diurnal cycles of LWP and GOES-derived cloud properties are compared in Fig. 5 for the  $V_{\text{eff}} = 0.10$  cases over Pt. Reyes to better understand the apparent dependency on scattering angle. The optical depth (Fig. 5a) decreases gradually after sunrise before increasing after noon. During the late afternoon,  $\tau$  suddenly rises and drops again before sunrise. The mean water droplet radius follows a similar pattern but is flatter during much of

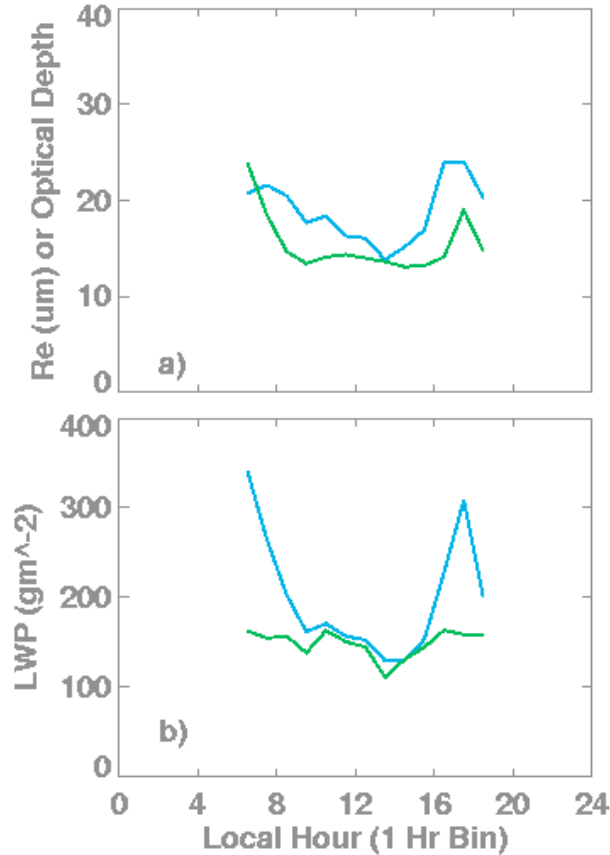


**Figure 5.** Mean surface and satellite-derived daytime cloud properties at Pt. Reyes as a function of local time. a) effective radius (green) and optical depth (blue) from GOES, b) LWP from GOES (blue) and MWR (green).

the day suggesting that  $\tau$  truly decreases until 1500 LT. This behavior is confirmed by the relatively good agreement between the MWR and VISST-derived LWP means (Fig. 5b) between 0900 and 1500 LT. The late afternoon peak in the satellite-derived products is coincident with a maximum ( $\sim 178^\circ$ ) in the scattering angle. Similar results (not shown) were found over the SCF except that the LWP was underestimated at the backscattering hour instead of overestimated. This difference is likely due to the occurrence of a larger SZA at Pt. Reyes compared to the 1400-LT backscatter maximum at the SCF. Thus, both scattering angle and SZA must be considered.

Figure 6 shows the mean differences between the GOES- and MWR-derived LWP as a function of SZA at Pt. Reyes and the SCF. In general, the results indicate that overestimation of LWP is not a significant problem until the SZA exceeds values around  $60^\circ$ . This finding is consistent with the SZA dependence of  $\tau$  for marine stratus clouds reported by Loeb and Coakley (1998). This effect is likely due to the 3-dimensional effects of actual clouds. Even “flat” stratus clouds have undulations and bumps that cast shadows and concen-

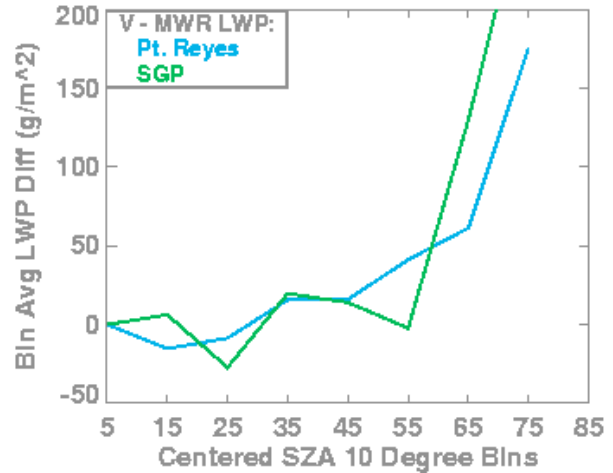


**Figure 6.** Average LWP differences between VISST and MWR per  $10^\circ$  SZA bin.

trate the reflected radiation in certain directions. These effects diverge from the plane-parallel assumption used to interpret the radiances leading to the types of errors seen here because the shadowing effect increases with increasing SZA.

The scattering angle effects will vary with the SZA as suggested by the differences between the SCF and Pt. Reyes results. The droplet size distributions will have little impact on the SZA effect but should alter the scattering angle effects because the width and intensity of the glory depends on both particle size and distribution. As indicated in Figs. 2-4, the biases vary as a function  $V_{\text{eff}}$ , probably as a result of reduced errors in the backscatter direction.

To examine the variation of the LWP errors as a function of  $V_{\text{eff}}$ , the differences for each  $V_{\text{eff}}$  were averaged for each of the three sites. Tables 1-3 show the average differences and standard deviations of the differences for the SCF, Pt. Reyes, and Manus, respectively. The results are given for  $\text{SZA} < 80^\circ$  and  $70^\circ$  to see the impact of the SZA dependence seen in Fig. 6. When the averages include values for  $\text{SZA} < 80^\circ$  (B80), the biases are 2-3 times greater than when cases with SZA between  $70^\circ$  and  $80^\circ$  were eliminated (B70) except over Manus where only one case was eliminated. The values of B80 are minimized when  $V_{\text{eff}}$  is 0.20, 0.01, and 0.30 over the SCF, Pt. Reyes, and Manus, respectively. The corresponding minima for B70 occur for  $V_{\text{eff}} = 0.20, 0.01, \text{ and } 0.25$ . S80 for Manus was also lowest for  $V_{\text{eff}} = 0.25$ , and B80 was also very low, indicating that  $V_{\text{eff}} = 0.25$  was the best fit overall; however, there is a lack of sufficient samples to determine this definitively. The minima at  $V_{\text{eff}} = 0.01$  and  $0.02$  are surprising because such narrow distributions are unrealistic when considering in situ observations. To be more realistic, the true minima for SCF and Pt. Reyes should be sought for  $V_{\text{eff}} > 0.05$ .

**Table 1.** Mean VISST LWP biases relative to the SFC MWR. Bxx: bias ( $\text{gm}^{-2}$ ), %xx: bias in %, Sxx: standard deviation of difference ( $\text{gm}^{-2}$ ), where SZA < xx°. Best overall results shown in bold.

$V_{\text{eff}}$	B80	%80	S80	B70	%70	S70
0.01	19.5	10.9	<b>103.7</b>	5.5	3.1	<b>79.9</b>
0.02	20.5	11.5	104.1	6.1	3.4	80.1
0.05	23.2	13.0	106.1	8.2	4.6	80.9
0.10	26.5	14.8	109.4	10.7	6.0	82.4
0.15	28.5	15.9	113.0	11.8	6.6	83.8
<b>0.20</b>	<b>18.8</b>	<b>10.5</b>	115.4	<b>0.9</b>	<b>0.5</b>	80.9
0.25	29.8	16.6	121.6	11.1	6.2	86.1
0.30	29.4	16.4	125.3	9.9	5.5	87.2

**Table 2.** Same as Table 2, except for Pt. Reyes.

$V_{\text{eff}}$	B80	%80	S80	B70	%70	S70
<b>0.01</b>	<b>40.3</b>	<b>26.9</b>	85.5	<b>14.1</b>	<b>9.7</b>	<b>51.3</b>
0.02	41.6	27.7	<b>85.3</b>	15.4	10.6	51.3
0.05	46.9	31.3	87.2	20.0	13.8	51.8
0.10	56.4	37.6	91.5	27.7	19.1	53.5
0.15	65.1	43.4	96.7	34.7	24.0	55.9
0.20	69.8	46.5	105.4	37.2	25.7	63.9
0.25	81.0	54.0	109.3	46.7	32.3	61.8
0.30	87.3	58.2	113.6	52.0	36.0	65.1

For the SCF, the minimum B70 and S70 is found for  $V_{\text{eff}}$  0.20. This would be consistent with the B80 minimum, suggesting that  $V_{\text{eff}}$  over the SCF is, on average, around 0.20. At Pt. Reyes, the minimum is found around  $V_{\text{eff}} = 0.05$  and increases monotonically with increasing  $V_{\text{eff}}$ .

These preliminary results suggest that the droplet spectra for the marine stratocumulus clouds are narrower than their continental counterparts at the SCF. Theoretically, the marine clouds should have narrower distributions because of fewer cloud condensation nuclei (CCN). However, in a review of in situ measurements, Miles et al. (2000) found that the relationship between  $V_{\text{eff}}$  and the air source region is relatively complicated and there appears to no significant difference between stratus formed in marine and continental air masses. For large mean droplet sizes, they found that the size distribution width is generally smaller for continental clouds, but is broader for marine stratus for small droplets. Hudson and Yum (1997) found that not all clouds have droplet size distributions that increase with droplet size, although their studies of large droplets of mean diameter > 15  $\mu\text{m}$  were found to broaden spectrally with increasing mean diameter. Other findings in their study however were that presence of increased droplet spectral width in marine stratus depended on a number of conditions. More detailed study of the Pt. Reyes cloud cases could reveal that the small  $V_{\text{eff}}$  found here could be appropriate in some cases.

**Table 3.** Same as Table 1, except for Manus.

<i>Manus</i>	B80	%80	S80	B70	%70	S70
0.01	-15.5	-19.3	49.5	-15.8	-19.0	51.2
0.02	-15.2	-18.8	49.6	-15.4	-18.6	51.2
0.05	-13.3	-16.4	49.5	-13.4	-16.2	51.1
0.10	-9.8	-12.2	49.3	-9.8	-11.9	50.9
0.15	-6.7	-8.3	49.1	-6.5	-7.8	50.7
0.20	-4.2	-5.2	49.1	-3.9	-4.7	50.7
<b>0.25</b>	-1.2	-1.5	<b>48.9</b>	<b>-0.7</b>	<b>-0.9</b>	<b>50.5</b>
0.30	<b>1.1</b>	<b>1.4</b>	49.1	1.7	2.0	50.7

Miles et al. (2000) also found that the spectral width for stratus clouds is highly variable and can introduce large errors into remote sensing retrievals. Politovich et al. (1993) found similar variability in cumulus clouds. This variability can be quantified by the range of biases seen in Tables 1-3. The range is larger over Pt. Reyes is largest suggesting that different types of clouds were found there. During the summer, the clouds are generally formed in marine air while during the stormier seasons, continental air can be drawn into the cloud systems. The SCF is a purely continental regime, which may explain the smaller variability in the biases. The initial results at Manus suggest that broad spectral distributions over ocean surfaces are common.

## 5. SUMMARY AND FUTURE STUDIES

The VISST retrievals using GOES-8, 9, and 10 data over various sites are preliminary, but indicate that LWP can be retrieved from satellite data in a reasonably accurate manner. This study showed that the effective variance used for the reflectance models in VISST can have a significant impact on the retrieval of LWP, and that the most appropriate  $V_{\text{eff}}$  can vary across cloud regimes. The greatest biases were found at high values of SZA. The VISST retrievals at high SZA should be improved, perhaps using empirical fits to data like those presented here.

Small  $V_{\text{eff}}$  was found to provide the best results for marine stratus cases, and a larger  $V_{\text{eff}}$  for continental. Further work is necessary to evaluate the source conditions for the clouds in association with the optimal value of  $V_{\text{eff}}$ . Conditions such as presence of drizzle can influence the spectral width of the droplet size distribution that would best characterize the cloud. More cases need to be analyzed in both marine and continental stratus, using various values of  $V_{\text{eff}}$ , to compare to ground-based MWR LWP. Other components of the VISST retrievals, such as the parameterization of visible reflectance, should be evaluated to determine whether the best values of  $V_{\text{eff}}$  found in this study, are indeed the most accurate.

## 6. ACKNOWLEDGEMENTS

The MWR data were obtained from the Atmospheric Radiation Measurement Program sponsored by the U.S. Department of Energy, Office of Science, Office of Biological and Environmental Research, Environmental Sciences Division. The GOES and RUC data was obtained from the Space Science and Engineering Center at University of Wisconsin-Madison. Some of the atmospheric profiles were generated by the CERES Meteorological, Ozone, and Aerosols group and obtained from the NASA Langley Atmospheric Sciences Data Center. This research was sponsored by ITF No. 214216-A-Q1 from Pacific Northwest National Laboratory, and Environmental Sciences Division of the U.S. Department of Energy Interagency Agreement DE-AI02-97ER62341.

## 6. REFERENCES

- Arduini, R. F., P. Minnis, W. L. Smith, Jr., J. K. Ayers, M.M. Khaiyer, and P.W.Heck: Sensitivity of Satellite-Retrieved Cloud Properties to the Effective Variance of Cloud Droplet Size Distribution. *Proc. of the 15<sup>th</sup> Annual ARM Science Team Meeting*, Daytona Beach, FL, March 14 – 18, 2005Ayers, J.K., P. Minnis, R. Palikonda, P.W.Heck, and R.F.Arduini: Evaluation of Cloud Properties Derived from Dual-View Satellite Data over the Continental United States. *Proc. of the 15<sup>th</sup> Annual ARM Science Team Meeting*, Daytona Beach, FL, March 14 – 18, 2005
- Hudson, J.G., and S. S. Yum, 1997: Droplet spectral broadening in marine stratus. *J. Atmos. Sci.*, **54**, 2642-2654
- Liljegren, J., E. Clothiaux, G. Mace, S. Kato, and X. Dong, 2001: A new retrieval for cloud liquid water path using a ground-based microwave radiometer and measurements of cloud temperature. *J. Geophys. Res.*, **106**, 14,485-14,500
- Loeb, N. G. and J. A. Coakley, 1998: Inference of marine stratus cloud optical depths from satellite measurements: Does 1D theory apply? *J. Climate*, **11**, 215-233.
- Miles, N. L., J. Verlinde, and E. E. Clothiaux, 2000: Cloud droplet distributions in low-level stratiform clouds. *J. Atmos. Sci.*, **57**, 295-311.
- Minnis, P., D. P. Garber, D. F. Young, R. F. Arduini, and Y. Takano, 1998: Parameterization of reflectance and effective emittance for satellite remote sensing of cloud properties. *J. Atmos. Sci.*, **55**, 3313-3339.
- Minnis, P., D. P. Kratz, J. A. Coakley, Jr., M. D. King, D. Garber, P. Heck, S. Mayor, D. F. Young, and R. Arduini, 1995: Cloud Optical Property Retrieval (Subsystem 4.3). "Clouds and the Earth's Radiant Energy System (CERES) Algorithm Theoretical Basis Document, Volume III: Cloud Analyses and Radiance Inversions (Subsystem 4)", *NASA RP 1376 Vol. 3*, edited by CERES Science Team, pp. 135-176.
- Minnis, P., L. Nguyen, D. R. Doelling, D. F. Young, W. F. Miller, and D. P. Kratz, 2002: Rapid calibration of operational and research meteorological satellite imagers, Part I: Evaluation of research satellite visible channels as references. *J. Atmos. Oceanic Technol.*, **19**, 1233-1249.
- Minnis, P., W. L. Smith, Jr., D. P. Garber, J. K. Ayers, and D. R. Doelling, 1995b: Cloud properties derived from GOES-7 for Spring 1994 ARM Intensive observing period using Version 1.0.0 of ARM satellite data analysis program. *NASA RP 1366*, 58 pp.
- Politovich, M. K., 1993: A study of the broadening of droplet size distributions in cumuli. *J. Atmos. Sci.* **50**, 2230-2244.
- Trepte, Q., Y. Chen, S. Sun-Mack, P. Minnis, D. F. Young, B. A. Baum, and P. W. Heck, 1999: Scene identification for the CERES cloud analysis subsystem. *Proc. AMS 10<sup>th</sup> Conf. Atmos. Rad.*, Madison, WI, June 28 – July 2, 169-172.
- Wielicki, B. A., et al., 1998: Clouds and the Earth's Radiant Energy System (CERES): Algorithm Overview. *IEEE Trans. Geosci. and Remote Sens.*, **36**, 1127-1141.